JACS
JOURNAL OF THE AMERICAN CHEMICAL SOCIETY
Communication
pubs.acs.org/JACS

Tin Oxide Dependence of the CO_2 Reduction Efficiency on Tin Electrodes and Enhanced Activity for Tin/Tin Oxide Thin-Film Catalysts

Yihong Chen and Matthew W. Kanan*

Department of Chemistry, Stanford University, 337 Campus Drive, Stanford, California 94305, United States

Supporting Information

ABSTRACT: The importance of tin oxide (SnO_x) to the efficiency of CO_2 reduction on Sn was evaluated by comparing the activity of Sn electrodes that had been subjected to different pre-electrolysis treatments. In aqueous $NaHCO_3$ solution saturated with CO_2, a Sn electrode with a native SnO_x layer exhibited potential-dependent CO_2 reduction activity consistent with previously reported activity. In contrast, an electrode etched to expose fresh Sn^0 surface exhibited higher overall current densities but almost exclusive H_2 evolution over the entire 0.5 V range of potentials examined. Subsequently, a thin-film catalyst was prepared by simultaneous electrodeposition of Sn^0 and SnO_x on a Ti electrode. This catalyst exhibited up to 8-fold higher partial current density and 4-fold higher faradaic efficiency for CO_2 reduction than a Sn electrode with a native SnO_x layer. Our results implicate the participation of SnO_x in the CO_2 reduction pathway on Sn electrodes and suggest that metal/metal oxide composite materials are promising catalysts for sustainable fuel synthesis.

Sustainable production of C-based fuels requires using renewable energy to power the reductive fixation of CO_2.[1,2] Coupling renewable electricity to an electrolytic device is an attractive strategy for this goal because it enables the use of multiple renewable energy sources and independent optimization of catalysis.[3] Solid oxide electrolytic cells reduce CO_2 to CO efficiently at high current densities but require operating temperatures of 750−900 °C and cannot access other products.[4,5] Efficient electrolytic fuel synthesis at lower temperatures (ambient to 100 °C) could dramatically simplify and lower the cost of renewable-to-fuel conversion. The principal obstacle to this goal is the development of a suitable CO_2 reduction catalyst. Recent promising approaches have demonstrated that energetically efficient CO_2 reduction can be achieved at low current densities by using pyridine as a soluble electrocatalyst[6] or by using an ionic liquid electrolyte.[7] However, a catalyst that is efficient at high current density and amenable to long-term use in an electrolytic device remains elusive.

Metal electrodes have been the focus of extensive CO_2 electroreduction studies in aqueous solutions at ambient temperature.[8−10] Sn has attracted considerable interest because it is one of the most active metals and its low cost is amenable to large-scale use.[11−14] Despite its appeal relative to other electrodes, the energy efficiency of Sn is too low for practical electrolysis. Sn is reported to require at least 0.86 V of overpotential to attain a CO_2 reduction partial current density of 4−5 mA/cm^2 in an aqueous solution saturated with 1 atm CO_2.[8] It is generally assumed that the bare Sn surface is the catalytically active surface for CO_2 reduction. The large overpotential required for CO_2 reduction is thought to result from the barrier associated with the initial electron transfer to form a $CO_2^{\bullet-}$ intermediate that is poorly stabilized by the Sn surface. This mechanistic scenario is commonly invoked for many metal electrodes.[9,15,16] However, SnO and SnO_2 form rapidly on the surfaces of Sn exposed to air.[17] Although the potentials required for CO_2 reduction are past the standard reduction potentials for these oxides, metastable metal oxides are known to persist on electrode surfaces during cathodic reactions.[18−20] Furthermore, the reported catalytic activities of Sn electrodes vary significantly, and a variety of electrode pretreatments have been employed in different studies, suggesting that the activity is sensitive to the condition of the surface.[20−22] On the basis of these observations, we hypothesized that SnO_x participates in the CO_2 reduction pathway on Sn electrodes by providing chemical functionality that stabilizes the incipient negative charge on CO_2 or by mediating the electron transfer directly. Here we show that SnO_x is essential for CO_2 reduction catalysis on Sn by demonstrating that removal of SnO_x from a Sn electrode results in nearly exclusive H_2 evolution activity. This insight has subsequently been applied to prepare a composite Sn/SnO_x thin-film catalyst that exhibits greatly enhanced CO_2 reduction activity relative to a typical Sn electrode.

To evaluate the importance of SnO_x on the surface of Sn in CO_2 reduction, we compared the activity of Sn electrodes that had been etched in strong acid to the activity of untreated electrodes. In both cases, new pieces of high-purity Sn foil (99.998%) were used. The surface of the untreated foil was examined by X-ray photoelectron spectroscopy (XPS) to characterize the native SnO_x layer [Figure 1a and Figure S2 in the Supporting Information (SI)]. The high-resolution Sn $3d_{5/2}$ spectrum was fit to two peaks at 486.5 and 484.7 eV that correspond to $Sn^{4+/2+}$ (SnO_x) and Sn^0, respectively.[23] The ratio of the corrected peak areas for SnO_x and Sn^0 was 95:5, indicating the presence of a >5 nm native SnO_x layer.[24]

Received: November 18, 2011
Published: January 9, 2012

dx.doi.org/10.1021/ja2108799 | J. Am. Chem.Soc. 2012, 134, 1986−1989

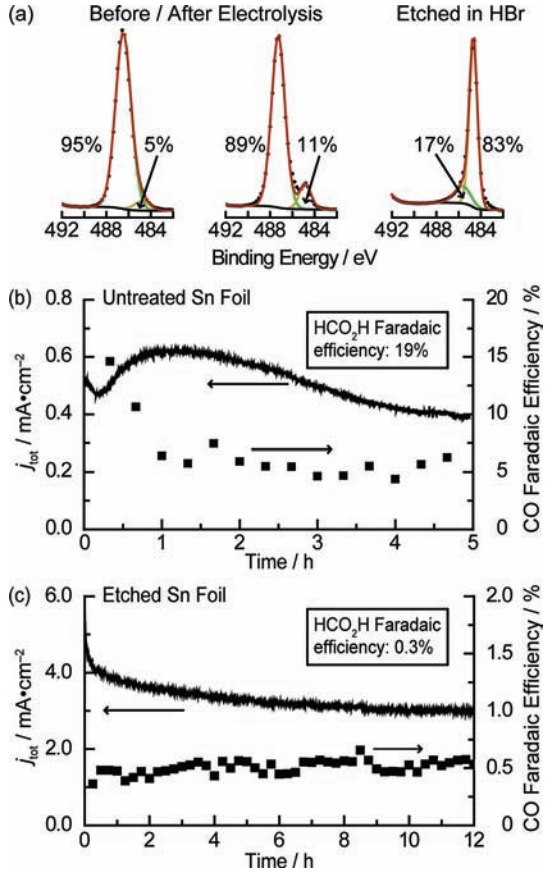

Figure 1. (a) XPS spectra of (left) untreated Sn foil before and after electrolysis and (right) Sn foil after etching in HBr. The red curves are combinations of two Gaussian/Lorentzian curves at 486.5 eV (green) and 484.7 eV (yellow). (b) Total current density vs time (solid line), CO faradaic efficiency vs time (■), and overall HCO_2H faradaic efficiency for untreated Sn at −0.7 V vs RHE in CO_2-saturated 0.5 M $NaHCO_3$. (c) Same data as in (b) for etched Sn.

Etched electrodes were prepared by immersing the Sn foil in 24% HBr at 90 °C for 10 min.[25] An XPS spectrum of the etched electrode taken immediately after removal from the HBr solution exhibited a SnO_x:Sn^0 ratio of 17:83 (Figure 1a). The residual oxide observed on this electrode is likely due to oxide regrowth in the brief exposure to air upon transfer to the XPS chamber, as assessed by independent XPS experiments with a sputtered electrode (see the SI). For electrolysis experiments, the etched electrodes were rinsed with deionized water at the conclusion of the etching procedure and used immediately to minimize oxide regrowth.

The electrolyses were performed in an H-cell in 0.5 M aqueous $NaHCO_3$ saturated with CO_2 ("$NaHCO_3/CO_2$") at a potential of −0.7 V vs the reversible hydrogen electrode (RHE; all potentials are referenced to this electrode). The headspace of the cathodic compartment was continuously purged with CO_2 into the sampling valve of a gas chromatograph (GC), enabling periodic quantification of the gas-phase products. Figure 1b shows the total geometric current density (j_{tot}) versus time and the faradaic efficiency for CO production at various time points for an untreated Sn electrode. The electrode exhibited a current density of 0.4−0.6 mA/cm^2 and a steady-state faradaic efficiency of 5−10% for CO. NMR analysis of the electrolyte at the conclusion of the experiment indicated a faradaic efficiency of 19% for HCO_2H; H_2 formation accounted for the remainder of the current. This CO_2 reduction activity is consistent with the best reported activity for Sn at −1.06 V,[8] taking into account the difference in overpotential. An electrode examined by XPS after a 12 h electrolysis at −0.7 V exhibited a SnO_x:Sn^0 ratio of 89:11, indicating that the native SnO_x layer was stable under the reduction conditions (Figure 1a).

Strikingly, an etched Sn electrode exhibited a much higher j_{tot} of 3−4 mA/cm^2 but very low faradaic efficiencies for production of CO (0.5%) and HCO_2H (0.3%) (Figure 1c). The higher j_{tot} likely reflects a larger electrochemical surface area due to etching. Despite the higher surface area, the geometric partial current density for CO_2 reduction was lower for the etched Sn electrode (24−32 μA/cm^2) than the untreated Sn electrode (92−140 μA/cm^2) because of the much lower faradaic efficiency. Very low (<1%) CO_2 reduction faradaic efficiencies on etched Sn were also observed over a range of potentials from −0.5 to −1.0 V (Table S1 in the SI). Thus, etched Sn is a moderately efficient H_2 evolution catalyst but is essentially inactive for CO_2 electroreduction. Similar results were obtained when Sn electrodes were etched by polarization at −3 V in HCl solution[26] instead of treatment with hot HBr solution (see the SI).

Together, the XPS and electrolysis results indicate that removal of the native SnO_x layer from a Sn electrode suppresses CO_2 reduction activity to such an extent that H_2 evolution accounts for >99% of the current density. The small residual CO_2 reduction activity observed on etched Sn likely reflects the growth of a small amount of SnO_x on the etched electrode before the start of electrolysis.

On the basis of these results, we hypothesized that the simultaneous deposition of Sn^0 and SnO_x on an electrode surface would result in a material with enhanced Sn−SnO_x contact that consequently would be a more active catalyst for CO_2 reduction than a typical Sn foil electrode with a native SnO_x layer. Accordingly, we sought electrodeposition conditions under which the hydrolysis of Sn^{2+} by cathodically generated OH^- would take place concurrently with the reduction of Sn^{2+} to Sn^0 (E^0 = +0.2875 V vs RHE). As described below, deposition on Ti electrodes under the same conditions used for CO_2 electroreduction proved to be particularly effective.

Figure 2a depicts the bulk electrolysis trace at −0.7 V in $NaHCO_3/CO_2$ electrolyte for a Ti cathode before and after the addition of 1 mM $SnCl_2$ to the electrolyte. Prior to the addition of Sn^{2+}, the Ti electrode exhibited a current density of ∼10 μA/cm^2 with very little detectable CO_2 reduction. Addition of Sn^{2+} resulted in a sharp rise in the current density to a steady-state value of ∼1.8 mA/cm^2 and the formation of a gray deposit on the electrode surface. The current density was stable for >10 h and corresponded to >85% CO_2 reduction, with H_2 evolution accounting for the remainder (see below). Nearly identical results were obtained when $Sn(OTf)_2$ was used instead of $SnCl_2$, indicating that Cl^- is not necessary for catalyst formation.

The composition and structure of the electrodeposited catalyst were characterized by a combination of scanning electron microscopy (SEM), XPS, and powder X-ray diffraction (PXRD). A catalyst was prepared via in situ deposition as described above and removed from the electrolyte 30 min after the addition of Sn^{2+}. SEM images of a Ti electrode before and after deposition showed the formation of a porous, particulate film with ∼100 nm diameter pieces atop a more uniform layer

dx.doi.org/10.1021/ja2108799 | J. Am. Chem.Soc. 2012, 134, 1986−1989

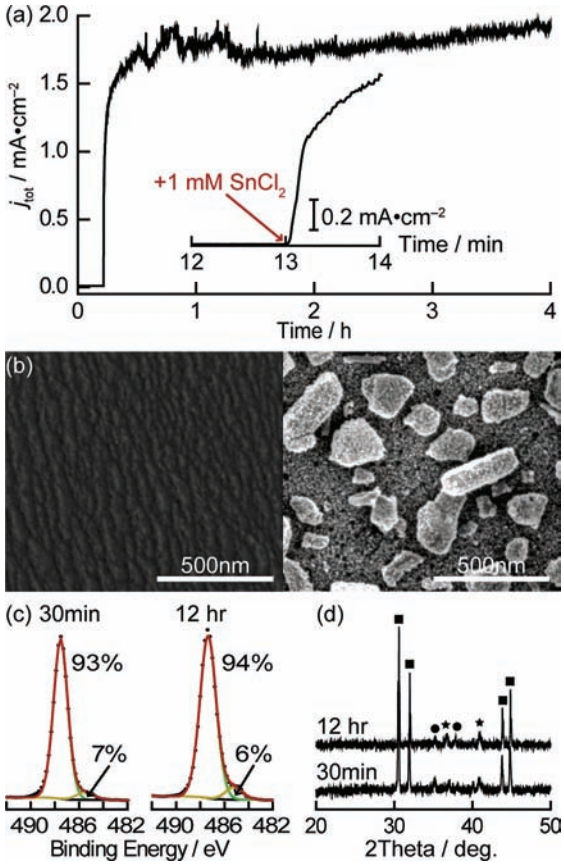

Figure 2. Sn/SnO_x thin-film catalysts. (a) Total current density trace for a Ti electrode at −0.7 V in $NaHCO_3/CO_2$ before and after addition of 1 mM Sn^{2+}. (b) SEM images of Ti foil (left) before and (right) after deposition of Sn/SnO_x. (c) High-resolution Sn $3d_{5/2}$ XPS spectra of a Sn/SnO_x catalyst removed (left) 30 min or (right) 12 h after the addition of Sn^{2+}. (d) PXRD patterns showing Sn^0 (■), SnO_2 (★), and Ti (●) peaks after 30 min or 12 h.

(Figure 2b). XPS analysis indicated a SnO_x:Sn^0 ratio of 93:7, similar to that observed for Sn foil electrodes with a native SnO_x layer (Figure 2c). In the PXRD pattern of this electrode, strong Sn^0 peaks were observed along with small peaks corresponding to SnO_2 (Figure 2d). The latter were absent for a Sn foil electrode with a native SnO_x layer (Figure S3). For comparison, a separate catalyst film was prepared and removed for analysis 12 h after the addition of Sn^{2+}. The XPS spectrum (Figure 2c) and PXRD pattern for this electrode are very similar to those of the sample removed after 30 min. Together, these results indicate that a composite Sn/SnO_x material was formed under the deposition conditions.

The electrodeposited catalyst (hereafter designated as "Sn/SnO_x") exhibited greatly enhanced CO_2 reduction catalysis relative to a typical Sn foil electrode with a native SnO_x layer. For both electrodes, CO, HCO_2H, and H_2 together accounted for >99% of the reduction products in $NaHCO_3/CO_2$ electrolyte. To compare the activities of Sn foil and Sn/SnO_x, we measured their partial current densities for CO and HCO_2H at selected potentials between −0.5 and −0.7 V (Figure 3a,b). These data were obtained by performing stepped-potential electrolyses with periodic quantification of the gaseous products by GC and removal of aliquots after each step for NMR analysis.[27]

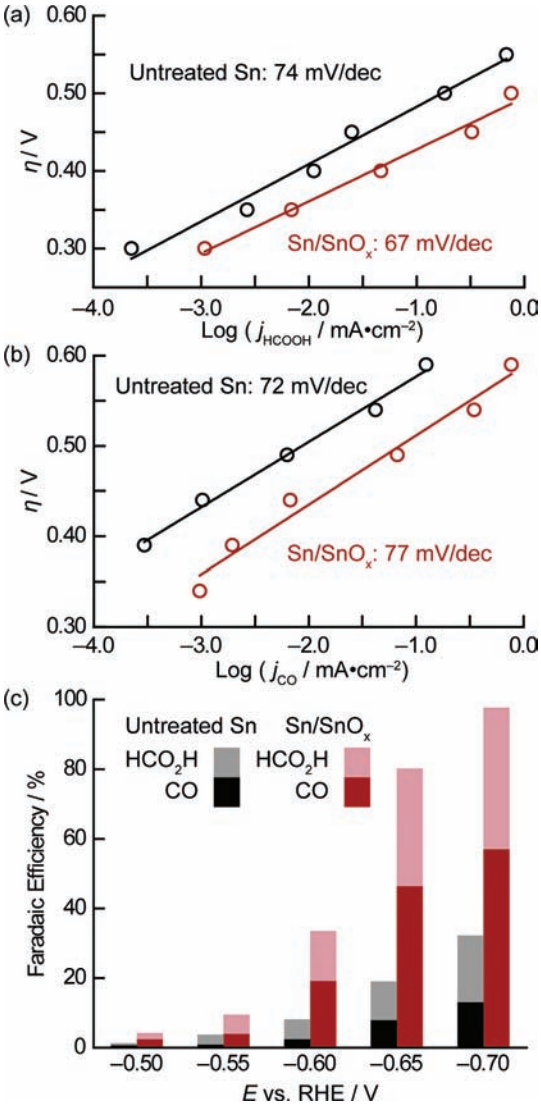

Figure 3. Comparison of CO_2 reduction catalysis for Sn foil and in situ-deposited Sn/SnO_x thin-film electrodes. (a, b) Tafel plots for production of (a) HCO_2H and (b) CO. (c) Faradaic efficiencies for HCO_2H and CO at various potentials. H_2 formation accounts for the remainder of the current.

For Sn foil, approximate Tafel slopes of 74 mV/dec and 72 mV/dec were observed for HCO_2H and CO production, respectively. Similar Tafel slopes were observed for production of HCO_2H (67 mV/dec) and CO (77 mV/dec) on Sn/SnO_x, but the geometric partial current densities were 7−8-fold higher than for Sn foil. The higher geometric current densities on Sn/SnO_x were not simply the result of a greater electroactive surface area, as indicated by cyclic voltammetry (see the SI) and the dramatic differences in faradaic efficiencies for Sn foil and Sn/SnO_x (Figure 3c). Over the range of potentials used for Tafel analysis, the CO faradaic efficiencies were 4-fold higher and the HCO_2H faradaic efficiencies 2−3-fold higher on Sn/SnO_x than on untreated Sn foil.[28]

The Tafel slopes for HCO_2H and CO production on both Sn foil and Sn/SnO_x are inconsistent with CO_2 reduction mechanisms that proceed through an initial rate-determining transfer of one electron to CO_2. Such a mechanism would result in a 118 mV/dec slope. The observed slopes are instead much closer to 59 mV/dec, which supports mechanisms

dx.doi.org/10.1021/ja2108799 | J. Am. Chem.Soc. 2012, 134, 1986−1989

involving a reversible transfer of one electron to CO_2 to form $CO_2^{\bullet-}$ prior to a chemical rate-determining step.[29] Possibilities for the chemical rate-determining step include protonation of $CO_2^{\bullet-}$ or migration to an alternative site on the electrode surface. Competing rate-determining steps, such as protonation at C versus O of $CO_2^{\bullet-}$, may determine the HCO_2H versus CO selectivity.

The Tafel data, combined with the absence of appreciable CO_2 reduction activity on etched Sn, suggest that SnO_x enables CO_2 reduction to occur by stabilizing $CO_2^{\bullet-}$. At present, we cannot determine whether reduction takes place at the interface between Sn^0 and SnO_x or on the SnO_x surface directly, as has been suggested in an early study on fluorine-doped tin oxide electrodes.[30] In the absence of SnO_x to stabilize $CO_2^{\bullet-}$, Sn^0 catalyzes only H_2 evolution because the electron transfer to CO_2 is prohibitively slow. The higher CO_2 reduction partial current density and faradaic efficiency on Sn/SnO_x relative to Sn foil with a native SnO_x layer are therefore indicative of a greater density of active sites for CO_2 reduction and a higher ratio of these sites to H_2 evolution sites for the in situ-deposited catalyst.

The CO_2 reduction activity of Sn/SnO_x, as indicated by the Tafel plots and faradaic efficiencies in Figure 3, compares favorably to those of all metal electrodes in aqueous electrolytes[8,31] with the exception of Au, which is comparably active initially but subject to rapid deactivation.[32] Improving CO_2 and ion mass transport by incorporating Sn/SnO_x in a flow cell and/or a gas diffusion electrode may enable an increase in the current density by 1−2 orders of magnitude without large overpotential increases.[11,12,14,33,34] Nevertheless, the use of Sn/SnO_x in a practical electrolytic device would require further improvements in its catalytic activity and demonstration of long-term stability. Elucidating the detailed mechanistic role of SnO_x in mediating electron transfer to CO_2 is an important objective toward this goal. Moreover, the importance of SnO_x to CO_2 reduction on Sn surfaces raises the possibilities that metal oxides may be involved in CO_2 reduction pathways on other metal electrodes and that the preparation of alternative metal/metal oxide composites may yield additional CO_2 reduction catalysts with superior activity.

■ ASSOCIATED CONTENT

Supporting Information

Experimental procedures, cyclic voltammetry, additional characterization data, and complete ref 3. This material is available free of charge via the Internet at http://pubs.acs.org.

■ AUTHOR INFORMATION

Corresponding Author

mkanan@stanford.edu

■ ACKNOWLEDGMENTS

We thank Stanford University and the Precourt Institute for Energy (PIE 10-008) for support of this work.

■ REFERENCES

(1) Olah, G. A.; Prakash, G. K. S.; Goeppert, A. *J. Am. Chem. Soc.* **2011**, *133*, 12881.

(2) Benson, E. E.; Kubiak, C. P.; Sathrum, A. J.; Smieja, J. M. *Chem. Soc. Rev.* **2009**, *38*, 89.

(3) Blankenship, R. E.; et al. *Science* **2011**, *332*, 805.

(4) Ebbesen, S. D.; Mogensen, M. *J. Power Sources* **2009**, *193*, 349.

(5) Barnett, S. A.; Zhan, Z.; Kobsiriphat, W.; Wilson, J. R.; Pillai, M.; Kim, I. *Energy Fuel* **2009**, *23*, 3089.

(6) Cole, E. B.; Lakkaraju, P. S.; Rampulla, D. M.; Morris, A. J.; Abelev, E.; Bocarsly, A. B. *J. Am. Chem. Soc.* **2010**, *132*, 11539.

(7) Rosen, B. A.; Salehi-Khojin, A.; Thorson, M. R.; Zhu, W.; Whipple, D. T.; Kenis, P. J. A.; Masel, R. I. *Science* **2011**, *334*, 643.

(8) Hori, Y.; Wakebe, H.; Tsukamoto, T.; Koga, O. *Electrochim. Acta* **1994**, *39*, 1833.

(9) Hori, Y. *Mod. Aspects Electrochem.* **2008**, *42*, 89.

(10) Whipple, D. T.; Kenis, P. J. A. *J. Phys. Chem. Lett.* **2010**, *1*, 3451.

(11) Oloman, C.; Li, H. *ChemSusChem* **2008**, *1*, 385.

(12) Whipple, D. T.; Finke, E. C.; Kenis, P. J. A. *Electrochem. Solid-State Lett.* **2010**, *13*, D109.

(13) Koleli, F.; Atilan, T.; Palamut, N.; Gizir, A. M.; Aydin, R.; Hamann, C. H. *J. Appl. Electrochem.* **2003**, *33*, 447.

(14) Agarwal, A. S.; Zhai, Y. M.; Hill, D.; Sridhar, N. *ChemSusChem* **2011**, *4*, 1301.

(15) Gattrell, M.; Gupta, N.; Co, A. *J. Electroanal. Chem.* **2006**, *594*, 1.

(16) Chandrasekaran, K.; Bockris, J. O. *Surf. Sci.* **1987**, *185*, 495.

(17) Hoflund, G. B.; Corallo, G. R. *Phys. Rev. B* **1992**, *46*, 7110.

(18) Zakroczymski, T.; Kleshnya, V.; Flis, J. *J. Electrochem. Soc.* **1998**, *145*, 1142.

(19) Rochefort, D.; Dabo, P.; Guay, D.; Sherwood, P. M. A. *Electrochim. Acta* **2003**, *48*, 4245.

(20) Frese, K. W. In *Electrochemical and Electrocatalytic Reactions of Carbon Dioxide*; Sullivan, B. P., Krist, K., Guard, H. E., Eds.; Elsevier: New York, 1993.

(21) Hori, Y.; Kikuchi, K.; Suzuki, S. *Chem. Lett.* **1985**, 1695.

(22) Jitaru, M.; Lowy, D. A.; Toma, M.; Toma, B. C.; Oniciu, L. *J. Appl. Electrochem.* **1997**, *27*, 875.

(23) Baronetti, G. T.; Demiguel, S. R.; Scelza, O. A.; Castro, A. A. *Appl. Catal.* **1986**, *24*, 109.

(24) Powell, C. J.; Jablonski, A. *NIST Electron Inelastic-Mean-Free-Path Database*, version 1.2, SRD 71; National Institute of Standards and Technology: Gaithersburg, MD, 2010.

(25) Hsu, Y. S.; Ghandhi, S. K. *J. Electrochem. Soc.* **1980**, *127*, 1592.

(26) Baliga, B. J.; Ghandhi, S. K. *J. Electrochem. Soc.* **1977**, *124*, 1059.

(27) Sn/SnO_x catalysts were prepared in situ and used directly in electrolyses. Sn/SnO_x films exposed to air exhibited a dramatic reduction in the current density when subsequently used in electrolysis (see the SI). We hypothesize that insulating SnO_x layers rapidly form between the small particles constituting Sn/SnO_x in the presence of O_2.

(28) Addition of Sn^{2+} to the electrolyte resulted in a 2−3-fold increase in the total current density and a ∼2-fold increase in the CO faradaic efficiency in an electrolysis with an untreated Sn foil electrode (see the SI), consistent with the formation of Sn/SnO_x on the Sn substrate. Greater CO_2 reduction activity was obtained when Ti was used as the substrate instead of Sn, however.

(29) Gileadi, E. *Electrode Kinetics for Chemists, Engineers, and Materials Scientists*; Wiley-VCH: New York, 1993.

(30) Shiratsuchi, R.; Hongo, K.; Nogami, G.; Ishimaru, S. *J. Electrochem. Soc.* **1992**, *139*, 2544.

(31) Ikeda, S.; Hattori, A.; Ito, K.; Noda, H. *Electrochemistry* **1999**, *67*, 27.

(32) Noda, H.; Ikeda, S.; Yamamoto, A.; Einaga, H.; Ito, K. *Bull. Chem. Soc. Jpn.* **1995**, *68*, 1889.

(33) Li, H.; Oloman, C. *J. Appl. Electrochem.* **2007**, *37*, 1107.

(34) Hara, K.; Sonoyama, N.; Sakata, T. *Stud. Surf. Sci. Catal.* **1998**, *114*, 577.